

Table S1. Clinical characteristics and cancer prevalence among 226 participants in the Johns Hopkins Telomere Syndrome Study (2003-2022), supplementary to Figure 1

	Whole Cohort N = 226	Females N = 94 (41.6%)	Males N = 132 (58.4%)	P**
Age at Enrollment - mean (SD)	45.44 (19.47)	44.1 (18.17)	46.4 (20.37)	ns
Age at Enrollment - median (range)	50 (0.58, 81)	49 (1, 76)	51 (0.58, 81)	ns
Deceased as of data cutoff				
No	105 (46.5)	55 (58.5)	50 (37.9)	0.008
Unknown	60 (26.5)	20 (21.3)	40 (30.3)	
Yes	61 (27)	19 (20.2)	42 (31.8)	
Sex				
Female	94 (41.6)	94 (100)	0 (0)	< 0.001
Male	132 (58.4)	0 (0)	132 (100)	
Mutant Gene				
<i>DKC1</i> -	17/226 (7.5)	0/94 (0)	17/132 (12.9)	< 0.001
<i>RTEL1</i>	25/226 (11.1)	11/94 (11.7)	14/132 (10.6)	ns
<i>TERT</i>	99/226 (43.8)	49/94 (52.1)	50/132 (37.9)	0.041
<i>TINF2</i>	3/226 (1.3)	2/94 (2.1)	1/132 (0.8)	ns
<i>TR</i>	27/226 (11.9)	18/94 (19.1)	9/132 (6.8)	0.006
<i>ZCCHC8</i>	3/226 (1.3)	0/94 (0)	3/132 (2.3)	ns
<i>NAF1</i>	5/226 (2.2)	4/94 (4.3)	1/132 (0.8)	ns
<i>PARN</i>	8/226 (3.5)	2/94 (2.1)	6/132 (4.5)	ns
Transplant status				
Any Transplant	51/226 (22.6)	16/94 (17)	35/132 (26.5)	ns
Received BMT	17/226 (7.5)	8/94 (8.5)	9/132 (6.8)	ns
Received Solid Organ Transplant	36/226 (15.9)	9/94 (9.6)	27/132 (20.5)	0.028
Cancer diagnoses*				
Any Cancer	35/226 (15.5)	7/94 (7.4)	28/132 (21.2)	0.005
Solid Tumor	14/226 (6.2)	1/94 (1.1)	13/132 (9.8)	0.009
MDS or AML	24/226 (10.6)	6/94 (6.4)	18/132 (13.6)	ns

**Cancer diagnoses did not include resected non-melanoma cutaneous malignancies, breast or prostate cancers which were not curated

**P-values were calculated using Student's *t*-test for comparisons of means, Wilcoxon rank sum test for comparisons of medians, and Fisher's exact test for comparison of categorical variables.

Table S2. Cumulative incidence of cancer by ages 50, 60 and 70, with 95% confidence intervals (supplementary to Figure 1)

	N	N events	Age 50	Age 60	Age 70	HR (95% CI)	P
Solid Tumors: Whole Cohort	226	14	0.03 (0.01, 0.06)	0.08 (0.03, 0.12)	0.09 (0.04, 0.14)		
Sex							
Females	94	1	0.01 (0, 0.03)	0.01 (0, 0.03)	0.01 (0, 0.03)		
Males	132	13	0.05 (0.01, 0.09)	0.11 (0.05, 0.18)	0.13 (0.06, 0.21)	8.01 (1.07, 60.26)	0.0432
Received Solid Organ Transplant							
No	190	9	0.03 (0, 0.06)	0.06 (0.01, 0.1)	0.07 (0.02, 0.12)		
Yes	36	5	0.03 (0, 0.08)	0.14 (0.01, 0.27)	0.14 (0.01, 0.27)	2.13 (0.74, 6.1)	0.1583
DKC1 Mutation-By-Sex							
No <i>DKC1</i> Mutation (Males)	115	9	0.01 (0, 0.03)	0.08 (0.02, 0.15)	0.1 (0.03, 0.18)	1.0 (Ref)	1.0 (Ref)
<i>DKC1</i> Mutation	17	4	0.37 (0.06, 0.67)	0.37 (0.06, 0.67)		7.02 (2.12, 23.3)	0.0014
No <i>DKC1</i> Mutation (Females)	94	1	0.01 (0, 0.03)	0.01 (0, 0.03)	0.01 (0, 0.03)	0.17 (0.02, 1.31)	0.089
MDS/AML: Whole Cohort	226	24	0.04 (0.01, 0.08)	0.13 (0.08, 0.19)	0.18 (0.11, 0.26)		
Sex							
Females	94	6	0.02 (0, 0.06)	0.08 (0, 0.16)	0.15 (0.03, 0.26)		
Males	132	18	0.06 (0.01, 0.11)	0.16 (0.08, 0.24)	0.2 (0.11, 0.29)	1.69 (0.68, 4.23)	0.2603
MDS/AML: <i>DKC1</i> Mutation-By-Sex							
No <i>DKC1</i> Mutation (Males)	115	16	0.04 (0, 0.09)	0.15 (0.07, 0.24)	0.2 (0.1, 0.29)	1.0 (Ref)	1.0 (Ref)
<i>DKC1</i> Mutation	17	2	0.23 (0, 0.59)	0.23 (0, 0.59)		1.97 (0.41, 9.5)	0.4007
No <i>DKC1</i> Mutation (Females)	94	6	0.02 (0, 0.06)	0.08 (0, 0.16)	0.15 (0.03, 0.26)	0.63 (0.25, 1.58)	0.3197

Hazard ratios (HR) and P-values were estimated for differences in cancer incidence between patient groups using Fine and Gray's method. Cumulative incidence of cancer was estimated using age as a time scale, accounting for the competing risk of death in univariate analysis.

Table S3. Risk of solid tumors estimated by hazard ratio using two multi-variate competing risks regression models (supplementary to Figure 1)

	HR [95% CI]	P
<i>Model 1</i>		
Males v Females	7.55 (0.94, 60.43)	0.0568
Rec'd Solid Organ Transplant vs. Did Not	1.85 (0.63, 5.45)	0.264
<i>Model 2</i>		
Rec'd Solid Organ Transplant vs. Did Not	1.84 (0.55, 6.16)	0.3255
<i>DKC1</i> Mutation vs. No <i>DKC1</i> Mutation (Males)	6.93 (1.87, 25.68)	0.0038
No <i>DKC1</i> Mutation (Females) vs. No <i>DKC1</i> Mutation (Males)	0.18 (0.02, 1.46)	0.1089

Model 1 includes sex and receipt of a solid organ transplant or not.

Model 2 includes sex-by-*DKC1* mutation groups and receipt of a solid organ transplant or not.

Figure S1

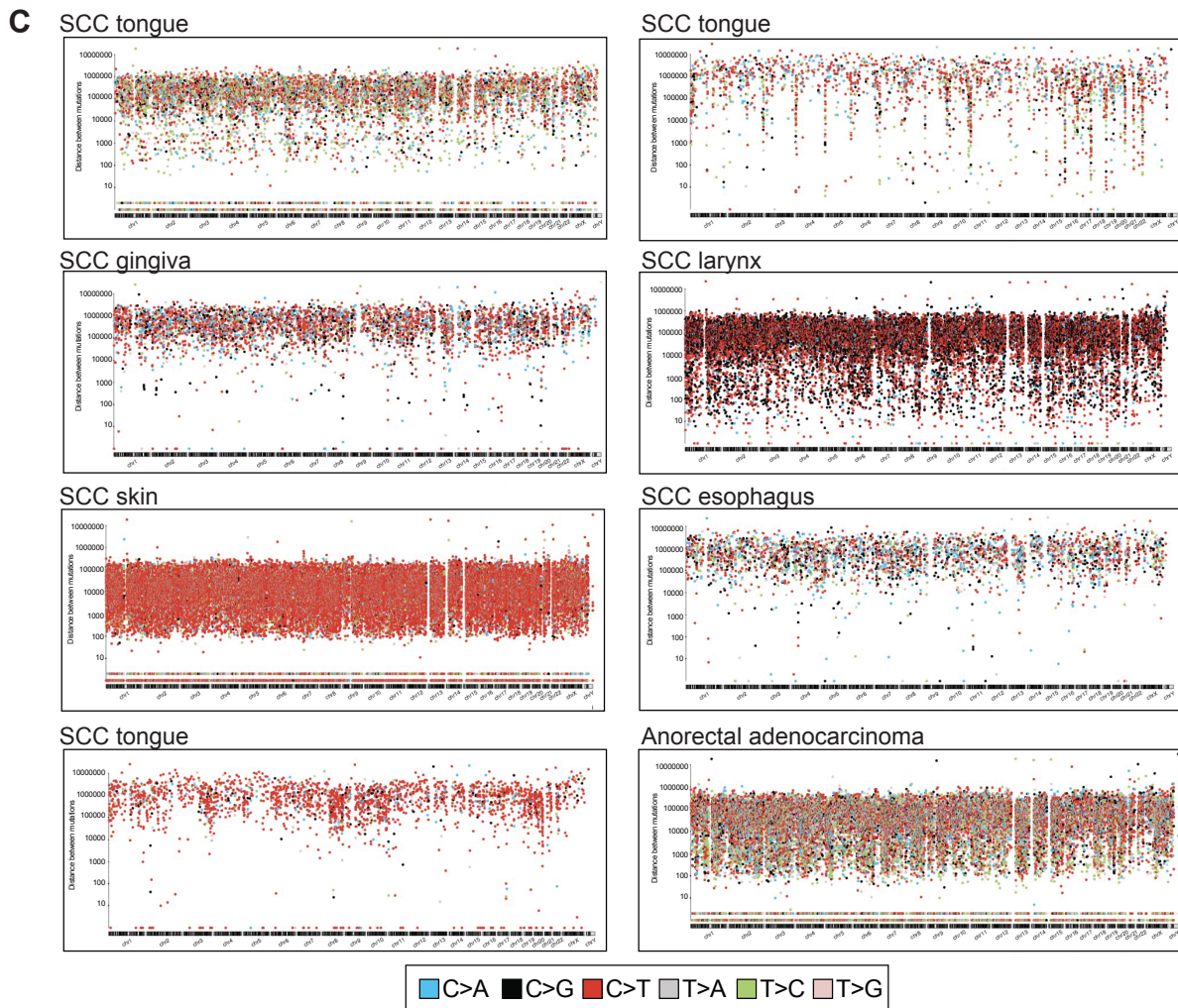
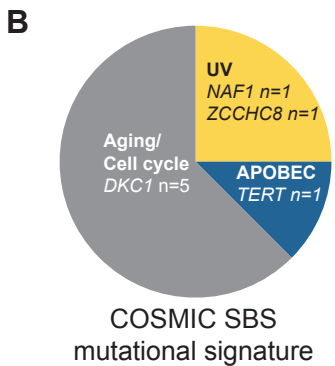
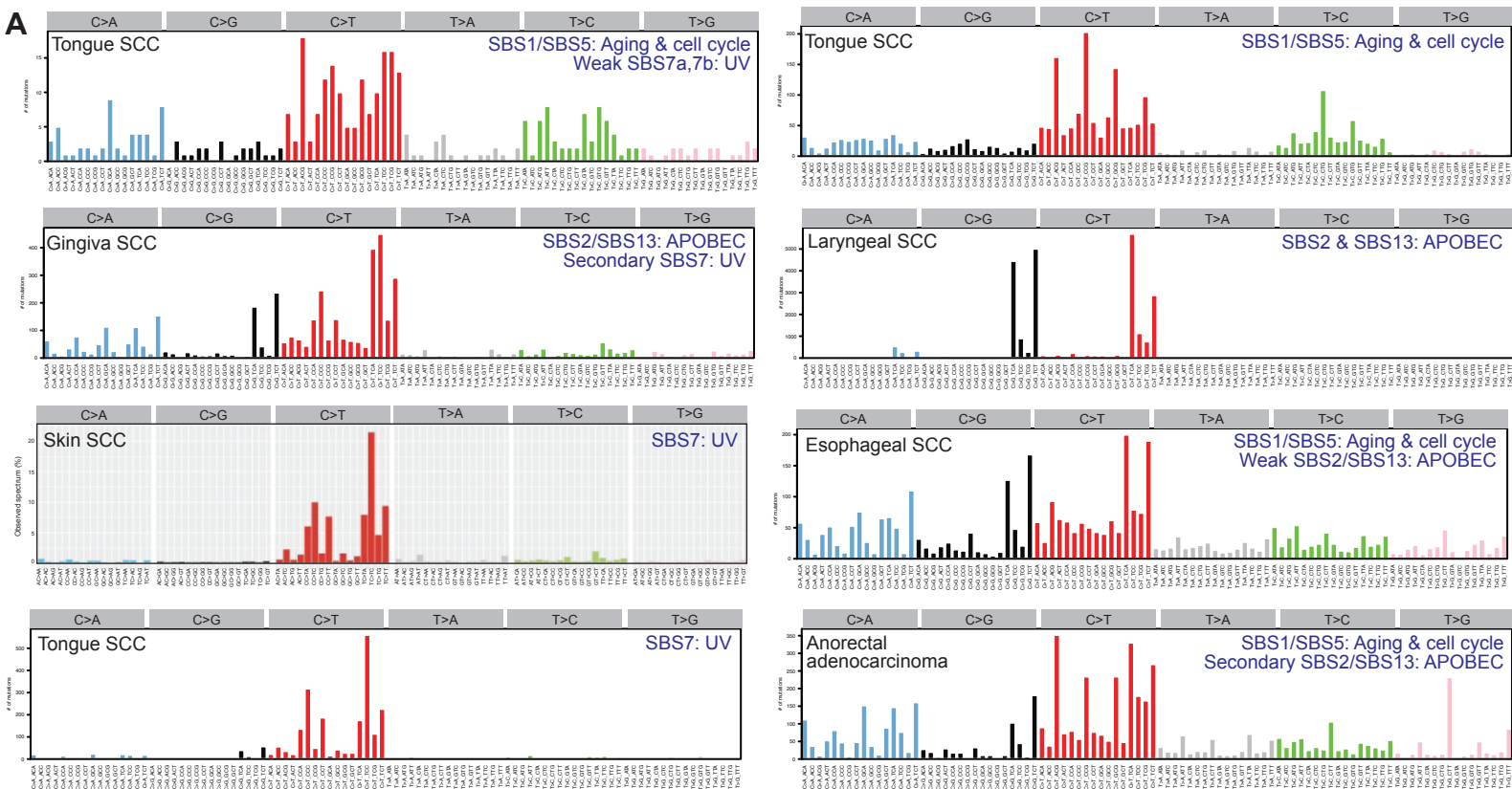


Figure S1. COSMIC single base substitution (SBS) mutational signatures and rainfall plots of 8 solid tumors derived from individuals with short telomere syndromes (supplementary to Figure 2).

A. Each mutational signature plot shows the distribution of mutations across the six potential types of substitutions generated by Mutalisk. Mutational signature analysis resulted in cosine score values above 0.90. Signatures were further analyzed using SigProfilerSingleSample and the concordant, predominant signature is annotated for each tumor in addition to any secondary or weaker signatures, if present. Weaker signatures were defined as less than 10% of the subtype detected and secondary as greater than or equal to 10% but less than the predominant signature.

B. Distribution of SBS mutational signature by germline mutant gene.

C. Rainfall plot analysis of kataegis focal hypermutability pattern analyzed by high pass whole genome sequencing. Each panel represents one tumor's analysis. Each dot represents a somatic single nucleotide variant, and dots are ordered on the horizontal axis according to genomic position. The vertical axis indicates the genomic distance between consecutive variants. None of the plots display a clustering of mutations over a 2 kb-sized DNA region as is characteristic of kataegis. All the plots were generated using a Bambino-based variant calling pipeline, except the squamous cell cancer of the skin plot which was generated using Mutect2 due to high background noise.

Figure S2

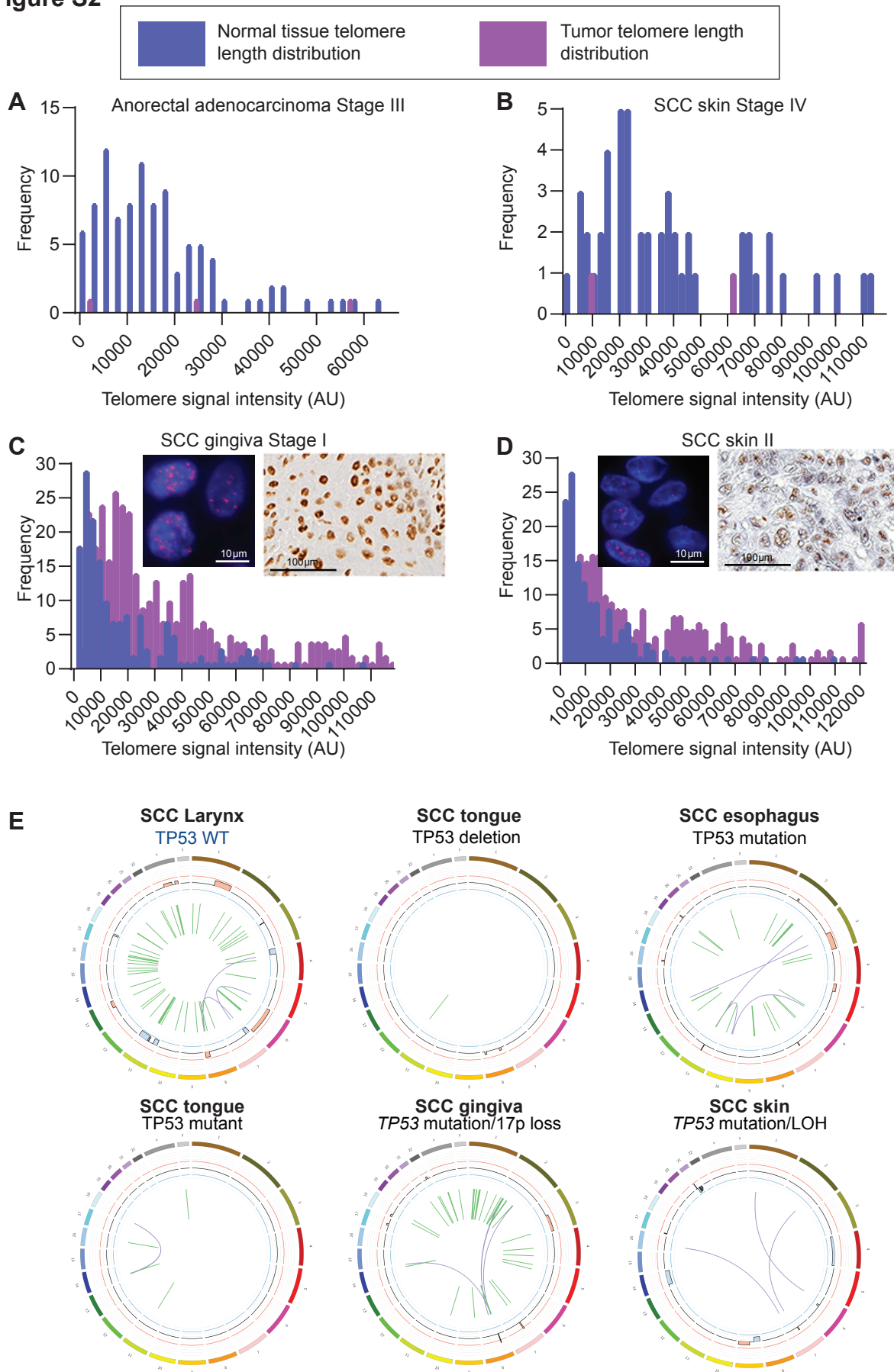


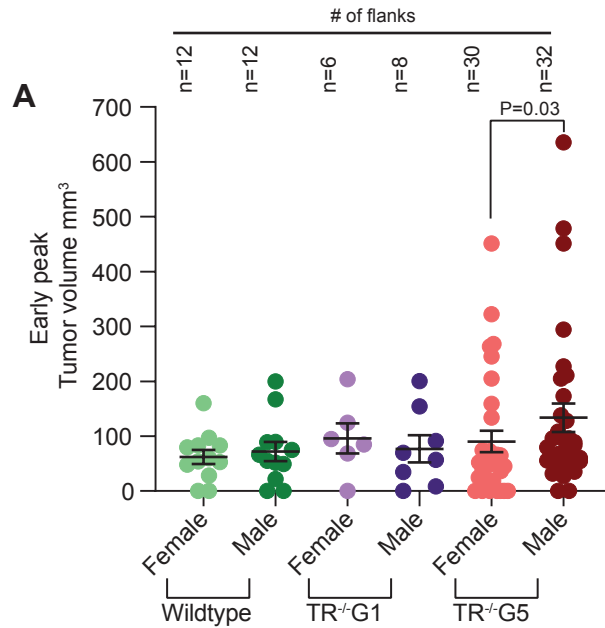
Figure S2. Telomere length distribution by quantitative in situ hybridization (Q-FISH) and circos plots of genomic alterations (supplementary to Figure 2).

A-B. Distribution of two tumors where the telomere length in the tumor had a very low signal, below detection in most cells, relative to adjacent normal tissue. These individuals had advanced stage disease.

C-D. Two tumors which have a longer telomere signal relative to adjacent normal tissue. Immunofluorescent inset panels show no evidence of ultrabright telomere foci characteristic of the alternative lengthening of telomeres (ALT) mechanism. In parallel, immunohistochemistry insets of the same respective tumors show retained ATRX staining in both tumors suggesting the longer telomeres were maintained via an ATRX-independent mechanism.

E. Genomic circos plots displaying somatic structural variants as well as greater than 3 Mb copy number variants detected using Illumina whole genome sequencing. Each circos plot is labelled by the cancer type and *TP53* status above. Circos plots for 6 tumors are shown with remaining 2 tumors shown in Figure 2I and 2J.

Figure S3



B Ova staining of tumors harvested from TR⁻G5 mice (representative of 8 tumors analyzed)

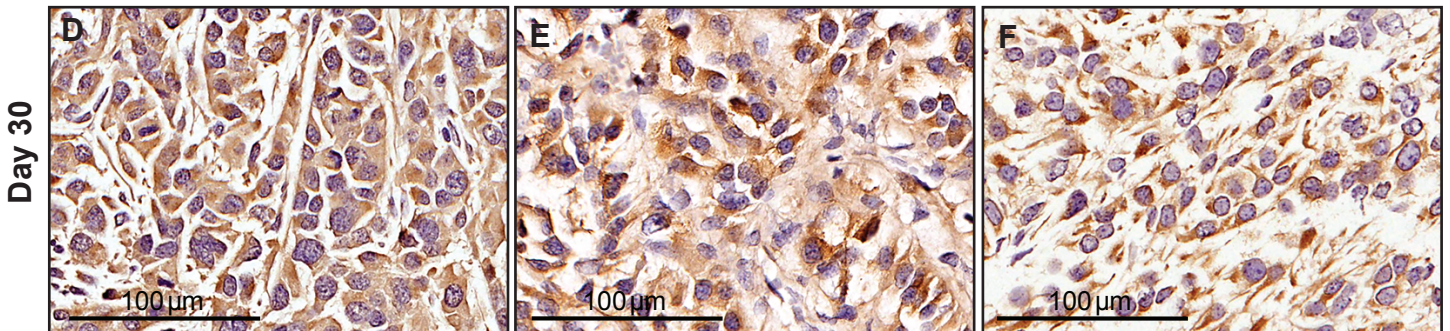


Figure S3. Tumor size by sex and ovalbumin immunohistochemistry of relapsed tumors (supplementary to Figure 4).

A. Maximum tumor volume in the first 10 days with each datapoint representing a single flank in each of the male and female mice studied. Mean and standard error bars are shown. P-value reflects two-sided Mann-Whitney test calculation.

B. Immunohistochemistry of tumors harvested after day 30 post-subcutaneous implantation that were harvested from short telomere mice (*mTR⁻G5*). Three representative images show retained cytoplasmic staining of the ovalbumin antigen (all 8 tumors showed a similar pattern). Tumors were harvested at a mean of 32 days post-implantation (range 24-47).